

# Multi-Dimensional Characterization of Mineral Abundance in Ordinary Chondrite Meteorites

Marina E. Gemma<sup>1,2,3,\*</sup> and Denton S. Ebel<sup>2,1,3</sup>

<sup>1</sup>Department of Earth and Environmental Sciences, Columbia University, New York, NY, USA

<sup>2</sup>Department of Earth and Planetary Sciences, American Museum of Natural History (AMNH), New York, NY, USA

<sup>3</sup>Lamont-Doherty Earth Observatory, Columbia University, Palisades, NY, USA; \*mgemma@amnh.org

Lamont-Doherty Earth Observatory  
COLUMBIA UNIVERSITY | EARTH INSTITUTE

AMERICAN MUSEUM  
OF NATURAL HISTORY



## Introduction

- Mineralogy within ordinary chondrites is highly variable, dependent on petrologic type [1], and the result of differing parent body processes [2].
- Quantifying representative mineralogy in meteorites often involves destructive techniques [3, 4] which sacrifice petrographic context.
- Traditional methods such as point counting do not provide a realistic estimation of modal mineralogy in these ordinary chondrite samples due to their fine-grained nature.

## Samples

- Twenty ordinary chondrite falls spanning the full range of petrologic types were sourced from the AMNH meteorite collection. Results from the following subset of LL chondrite samples are shared on this poster:
  - Parnallee (LL3.6)
  - Soko-Banja (LL4)
  - Tuxtuac (LL5)
  - Mangwendi (LL6)

## Task

- Combine the non-destructive methods of 3D computed tomography (CT) with 2D X-ray element intensity mapping of surfaces to quantitatively determine mineral modal abundances and variability across petrologic types of ordinary chondrites without losing petrographic context.
- Broader Goal:** Utilize precise mineral abundances in meteorites to quantitatively link laboratory spectroscopy of meteorites to that of asteroids to better understand parent body and asteroid compositions.

## Conclusions

- This method produces more precise abundances (characterization at the ~micron scale) than point counting and preserves petrographic context (unlike powder X-Ray Diffraction). This work is not only useful as a non-destructive method that preserves a sample's petrographic context, but also can be used to characterize laboratory spectroscopic measurements of the meteorite samples.
- Next steps involve improving the 2D mineral identification algorithm to better classify unknown pixels.

## References

- [1] McSween H. et al. (1991) *Icarus*, **90**, 107–116. [2] Jones R. H., et al. (2014) *Geochim. Cosmochim. Acta* **132**, 120–140. [3] Dunn T. et al. (2010) *Meteor. Planet. Sci.* **45**, 123–134. [4] Menzies O. et al. (2005) *Meteor. Planet. Sci.* **40**, 1023–1042. [5] Gastineau-Lyons H. et al. (2002) *Meteor. Planet. Sci.* **37**, 75–89. [6] Weisberg M. et al. (2006) *Meteorites and the Early Solar System*, 19–52. [7] Nakamura, T., et al. (2011). *Science*, **333**(6046), 1113–1116.

## Acknowledgements

The authors thank Henry Towbin and the staff at the AMNH Microscopy and Imaging and EPMA facilities for operation and analysis assistance. This work was supported by NASA Emerging Worlds grant NNX16AD37G (DE).

## Methods

### Step 1: 3-D Characterization

**Tool:** GE phoenix v|tome|x s 240  
**Sample:** 2-6 cm<sup>3</sup> bulk meteorite  
**Resolution:** 6-11 microns/voxel  
**Objective:** Characterize 3D structure of samples and determine the abundance of opaque phases

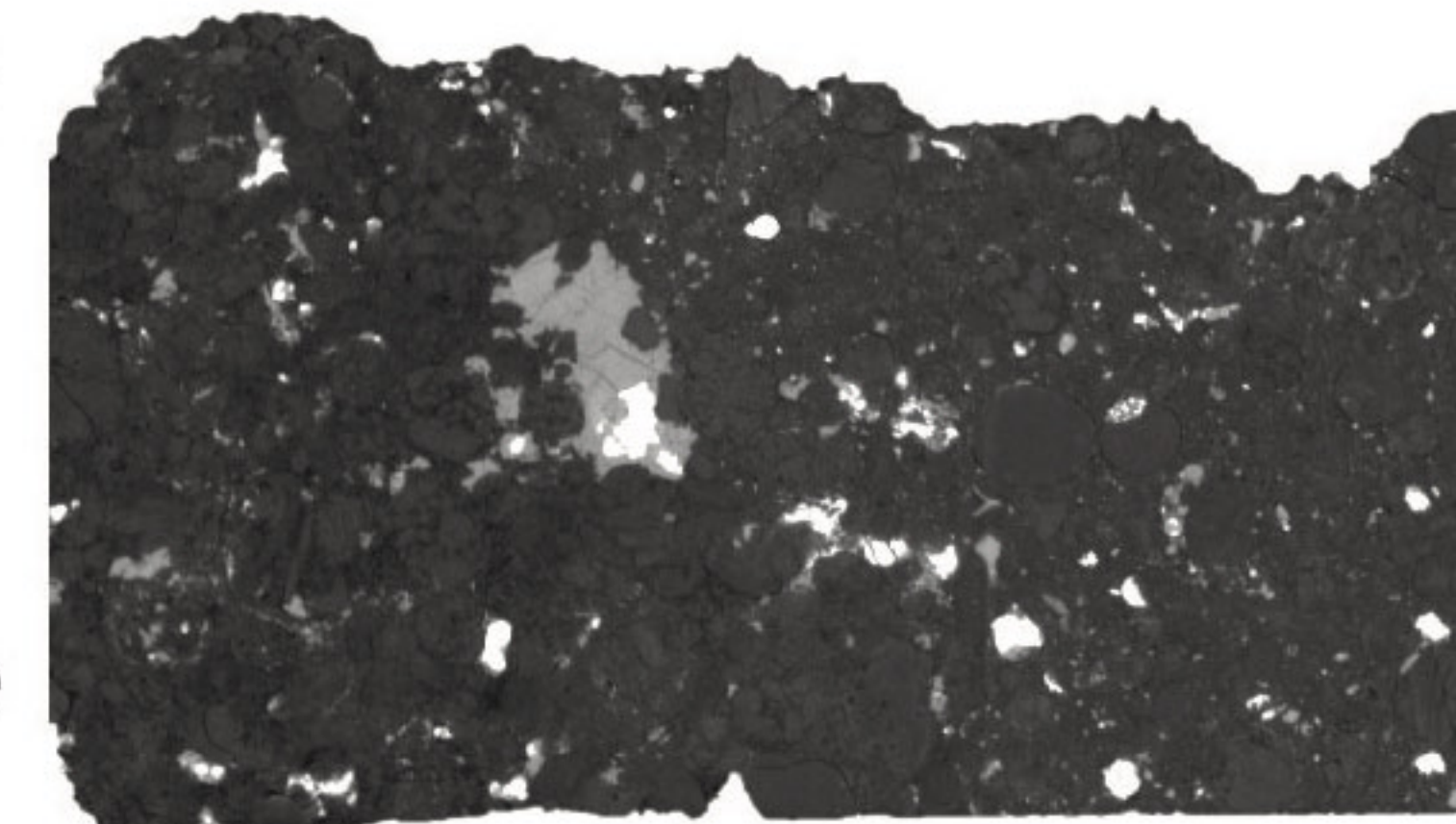


Figure 1a. 2D slice from 3D CT scan of Soko-Banja (LL4). Resolution = 8.8 microns/voxel. Major mineral phases in order of decreasing brightness: Metal, Sulfide, Pyroxene, Olivine.

### Step 2: 3-D Reconstruction

**Tool:** phoenix datos|x software  
**Objective:** Render and process 3D scan of meteorite sample



Figure 1b. 3D volume rendered from tiff stack of X-ray maps from the CT scan of Soko-Banja (LL4). Total volume = 4.13 cm<sup>3</sup>. Intact spherical chondrule visible on lower right, corresponds to circular chondrule in upper right of Fig. 1a.

### Step 3: 3-D Segmentation

**Tool:** VGstudio software  
**Objective:** Isolate mineral phases based on density, calculate total volume of sample and volume of opaque phases

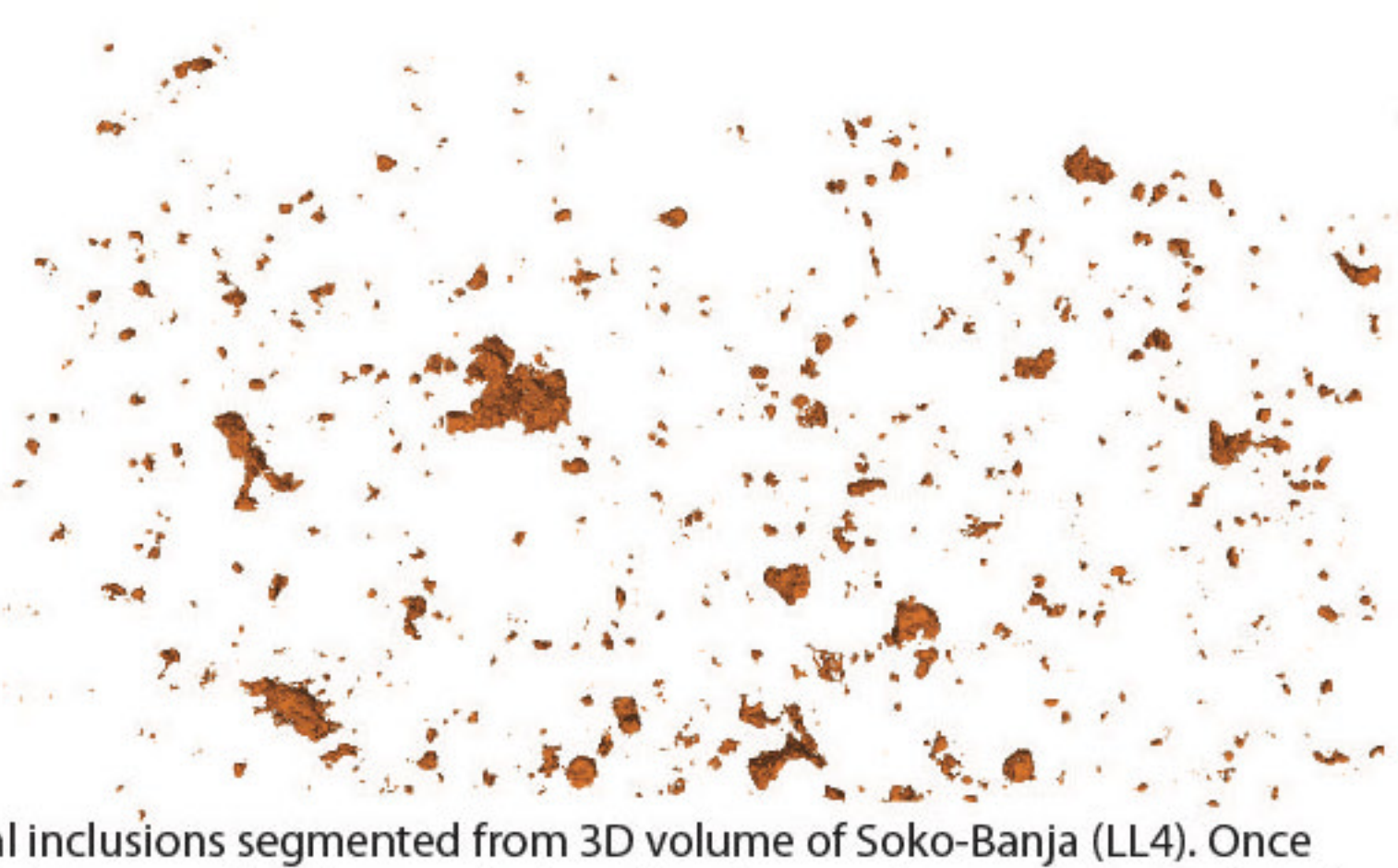


Figure 1c. Metal inclusions segmented from 3D volume of Soko-Banja (LL4). Once desired mineral phase is isolated, can calculate abundance of given phase in the volume.

### Step 4: 2-D X-ray Mapping

**Tool:** Cameca SX100 Electron Microprobe  
**Sample:** Thin or thick polished sections; mapped area of 0.6 cm<sup>2</sup> - 1 cm<sup>2</sup>  
**Resolution:** 4-6 microns/pixel  
**Objective:** Determine intensities of 10 major and minor elements (Mg, Si, Ca, Al, Fe, Ni, S, Ti, Cr, P)

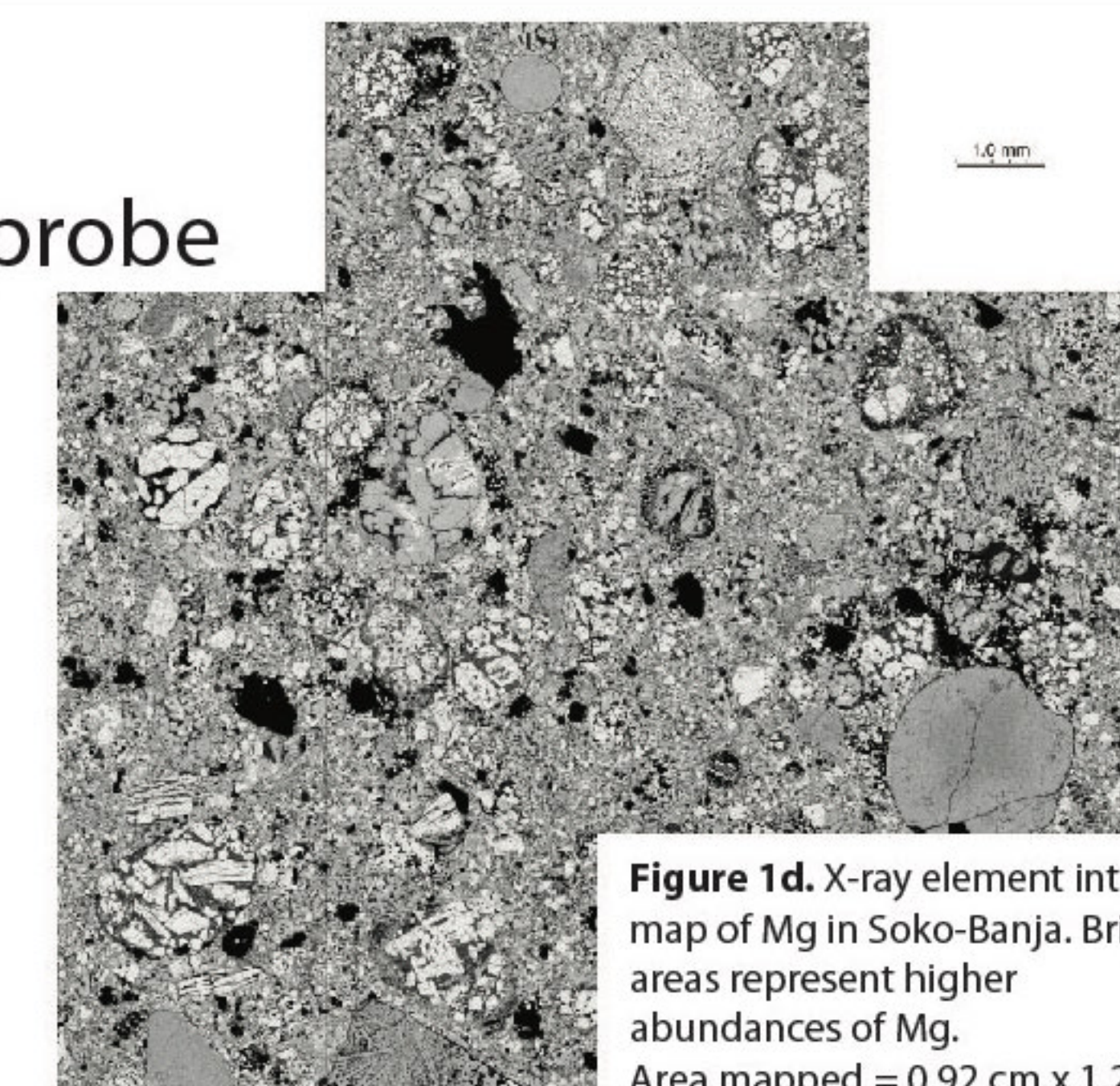


Figure 1d. X-ray element intensity map of Mg in Soko-Banja. Brighter areas represent higher abundances of Mg. Area mapped = 0.92 cm x 1.22 cm.

### Step 5: 2-D Composite Images

**Tool:** IDL software  
**Objective:** Qualitative representation of mineralogy in the sample, using combinations of mapped elements (e.g. MgCaAl, FeNiS, etc).

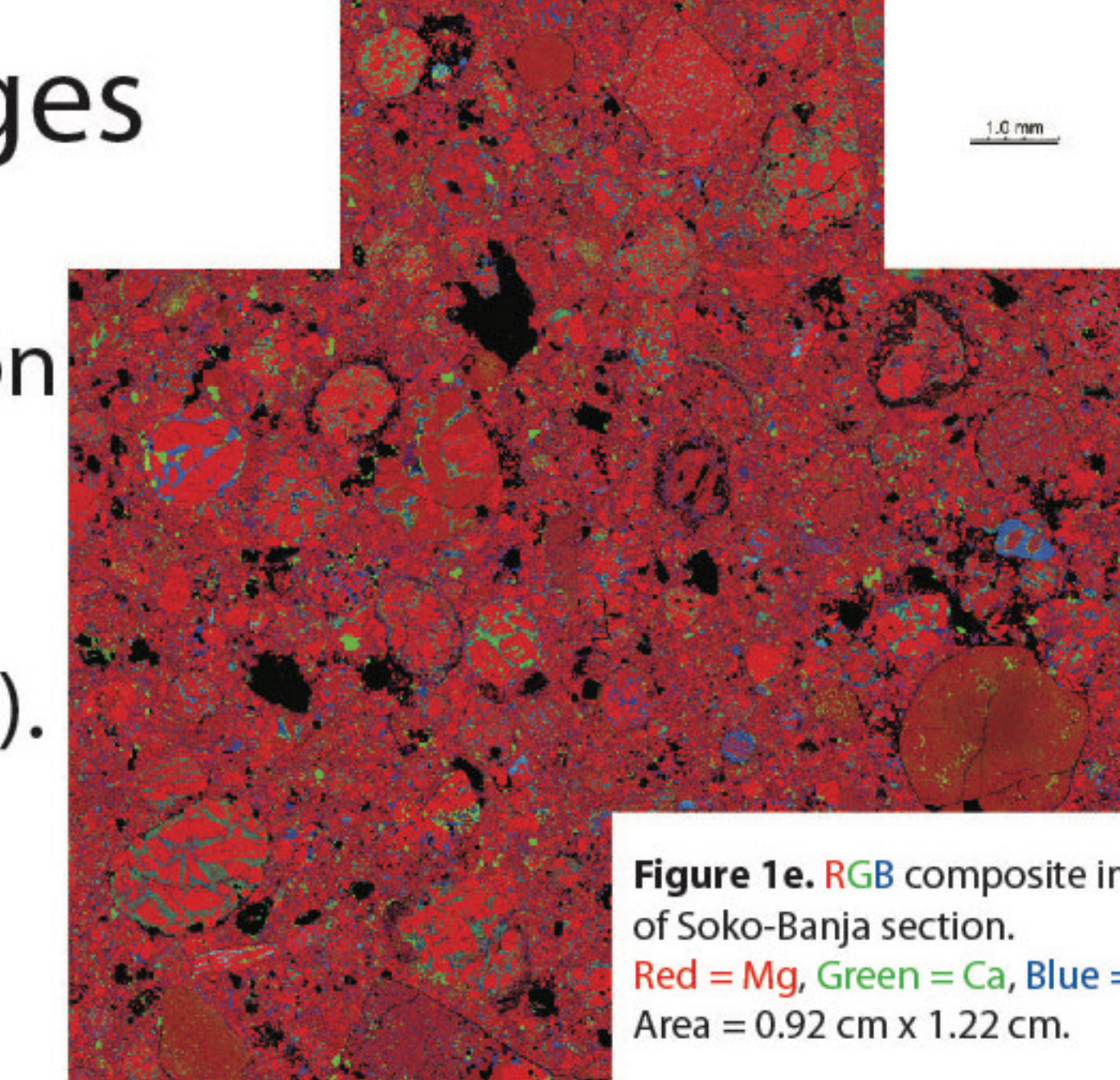


Figure 1e. RGB composite image of Soko-Banja section. Red = Mg, Green = Ca, Blue = Al. Area = 0.92 cm x 1.22 cm.

### Step 6: 2D Modal Abundance

**Tool:** IDL software  
**Objective:** Quantitative calculation of mineral abundances in the sample from element intensity maps.

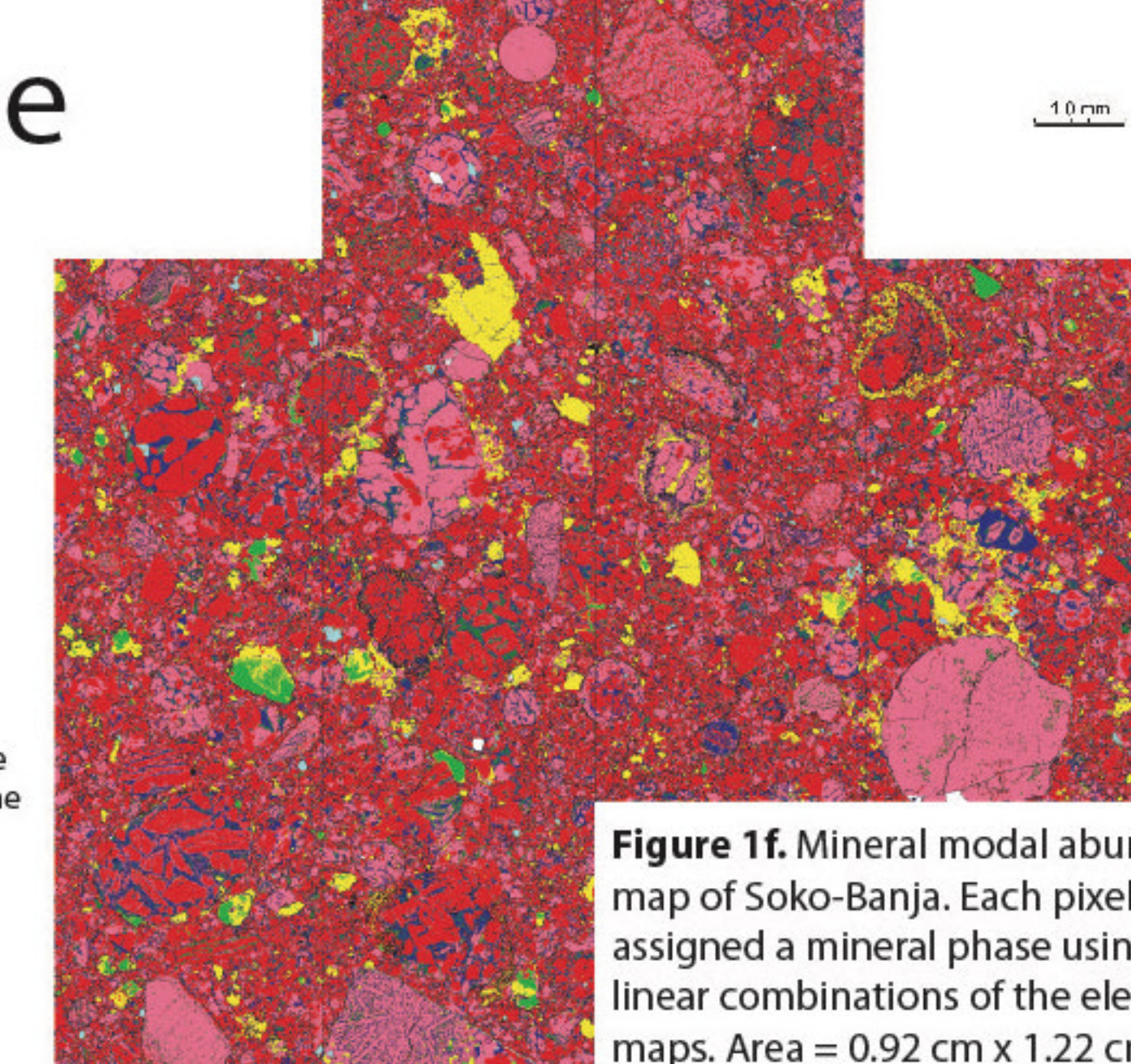


Figure 1f. Mineral modal abundance map of Soko-Banja. Each pixel was assigned a mineral phase using linear combinations of the element maps. Area = 0.92 cm x 1.22 cm.

## Results

- 2D vs. 3D:** 2D element mapping of a ~1 cm<sup>2</sup> sample surface area produces mineral abundances consistent with 3D bulk scans of a ~4 cm<sup>3</sup> parent sample.
  - Abundances of mineral phases in 2D and 3D are consistent to within 1% for equilibrated samples (types 4-6), and to within ~2% for the unequilibrated (type 3) samples (Figures 2 & 3).
  - 2D mapping of an area approximately 0.6 cm<sup>2</sup> - 1 cm<sup>2</sup> is representative of the bulk sample.**
- Calculated abundances are also consistent with existing literature on the compositions of ordinary chondrites.

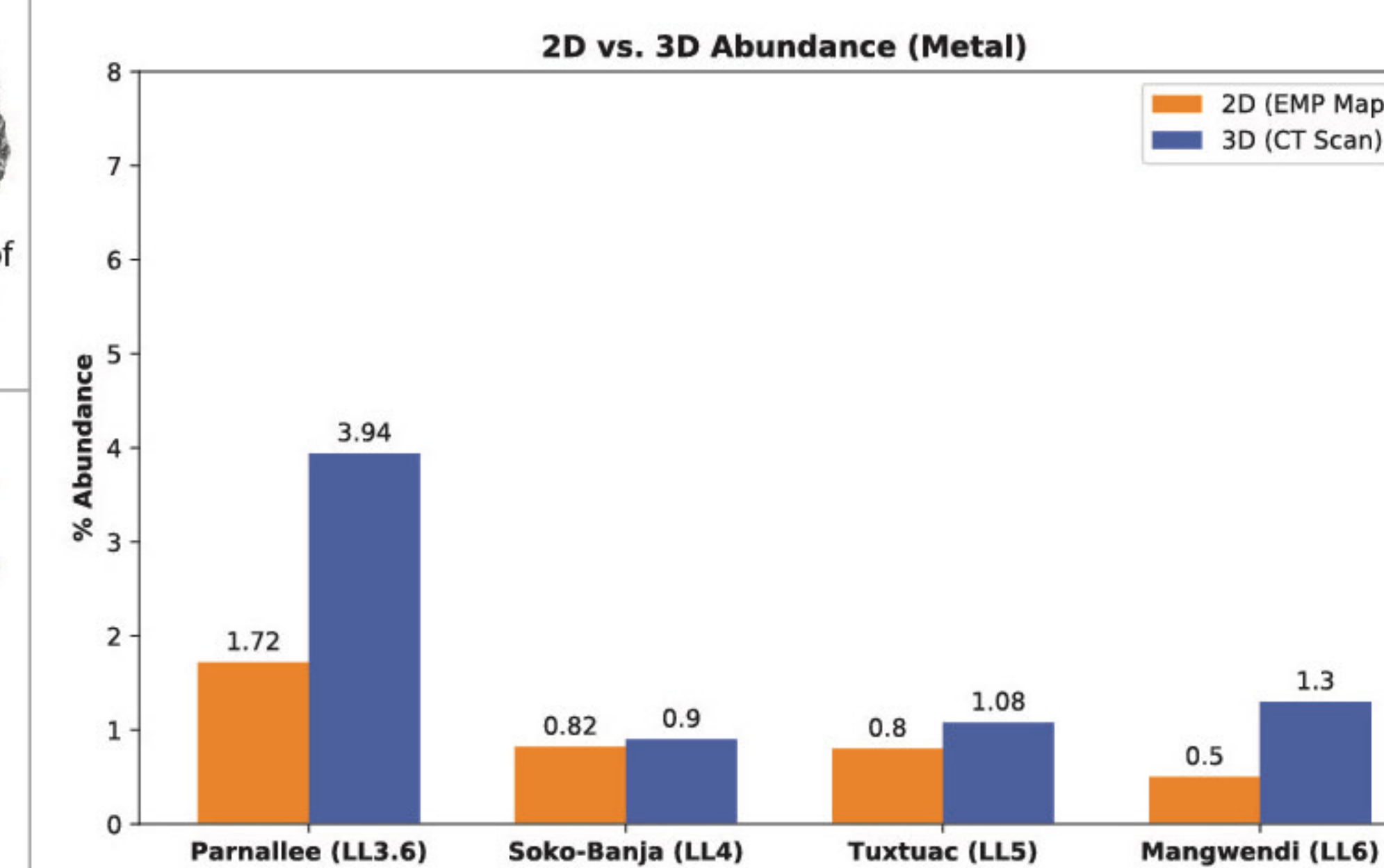


Figure 2. Comparison of metal abundances in 2D vs. 3D

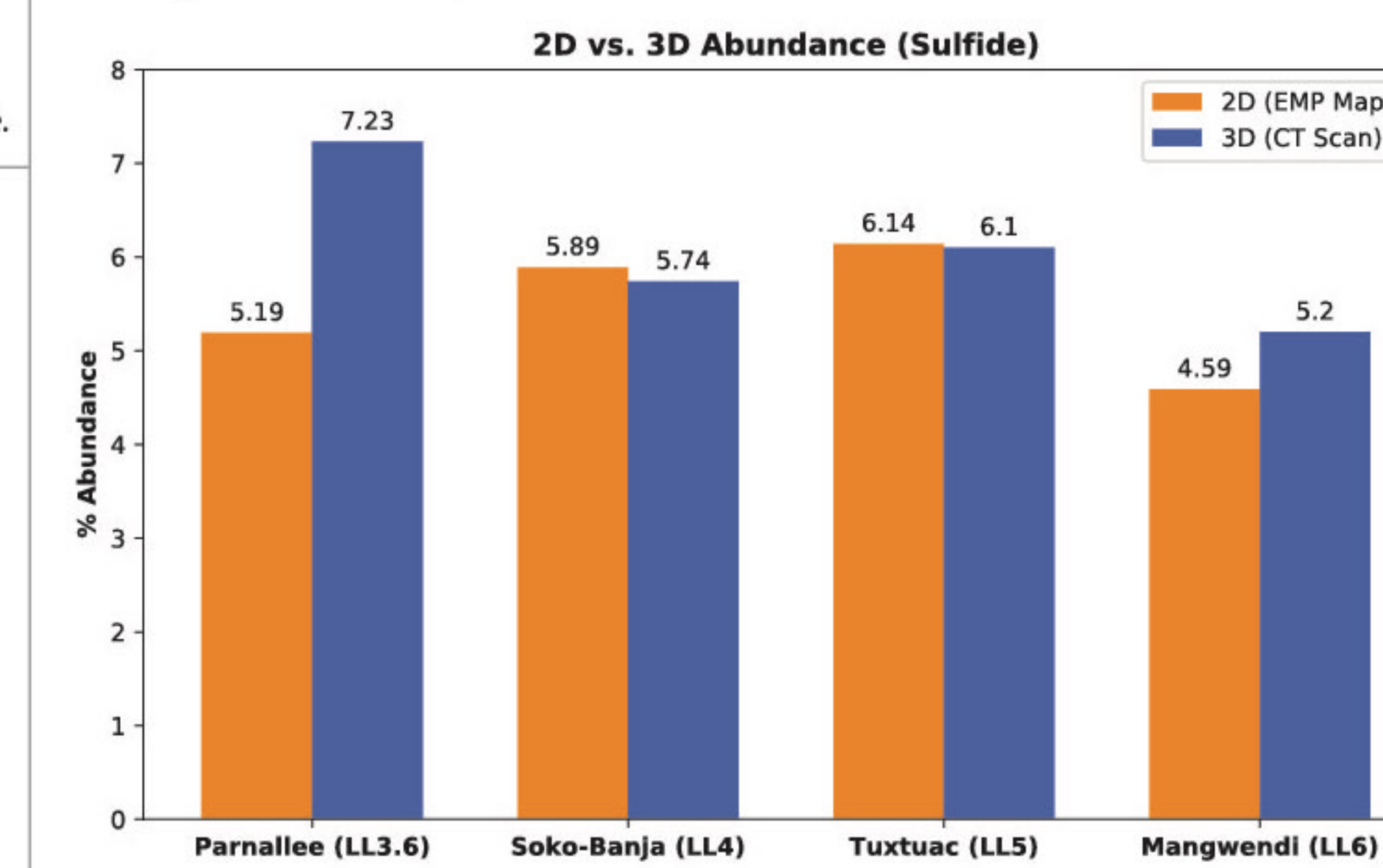


Figure 3. Comparison of sulfide abundances in 2D vs. 3D

**Table 1 (below).** Mineral modal abundances of LL ordinary chondrite samples from each petrologic type (3-6). Olivine and Ca-poor pyroxene are the most modally abundant phases in all samples. Metal values (kamacite + taenite) decrease as petrologic type increases, likely due to coarsening of metal inclusions as the degree of thermal metamorphism intensifies.

**Legend (Figures 4 & 5)**

- Chromite
- Ca-Phosphate
- Taenite
- Kamacite
- Ca-rich pyroxene
- Ca-poor pyroxene
- Glass
- Olivine
- Troilite (FeS)
- Hole
- Unknown

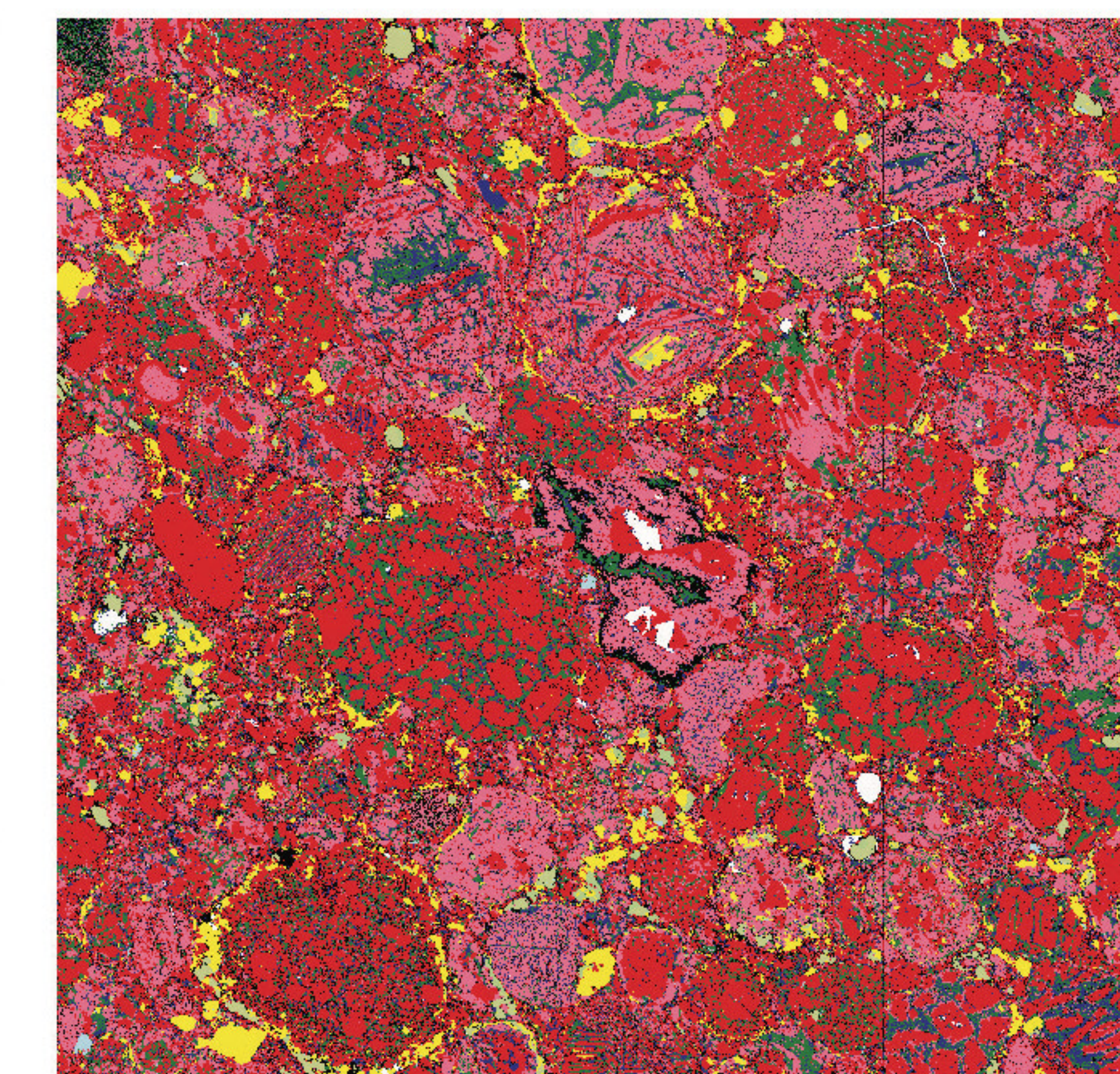


Figure 4. Mineral modal abundance map for Parnallee (LL3.6). Mapped Area = 0.6 cm<sup>2</sup>.

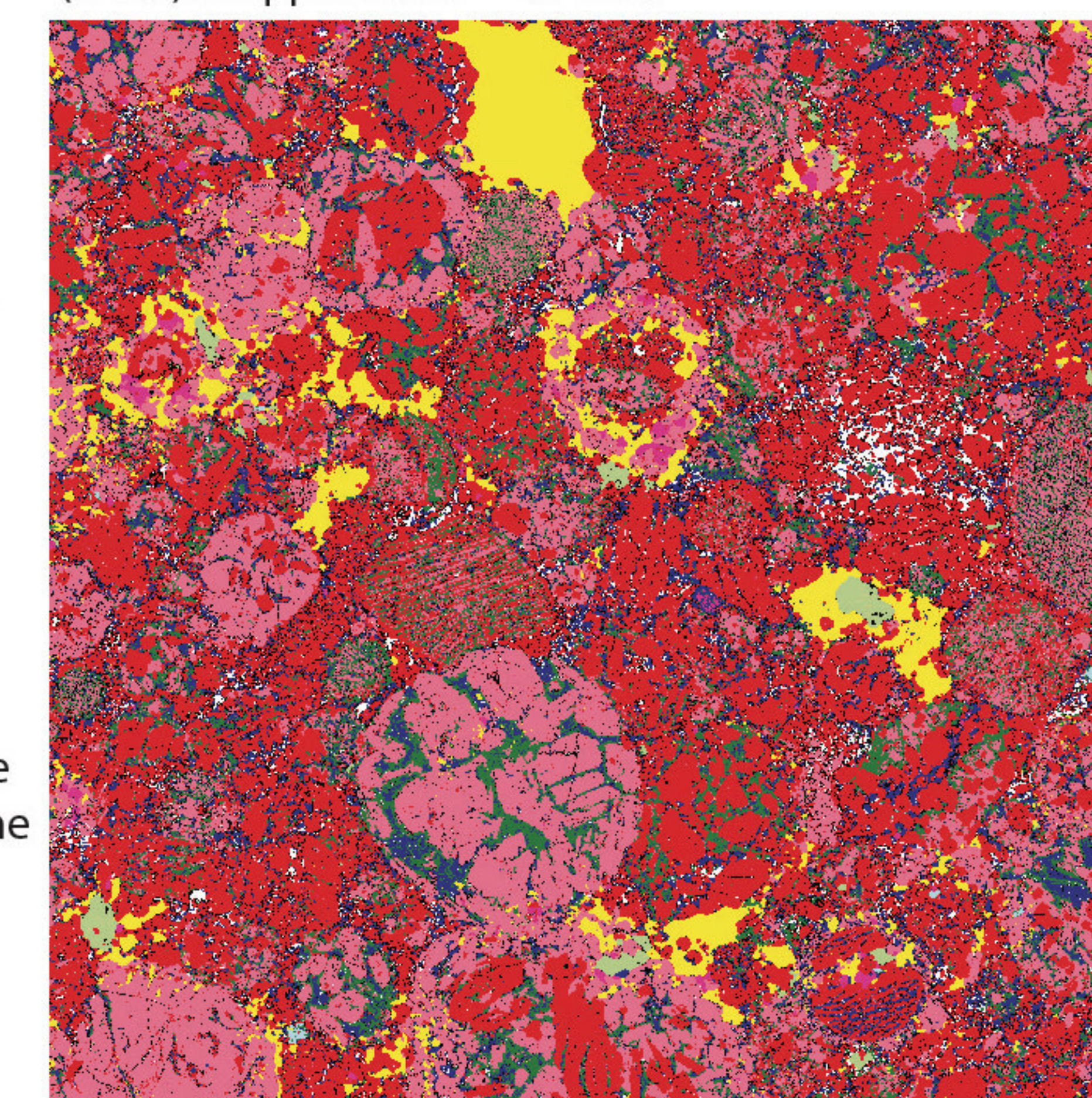


Figure 5. Mineral Modal Abundance Map for Tuxtuac (LL5). Mapped Area = 0.6 cm<sup>2</sup>.

Mineral Phase	Parnallee (LL3.6)	Soko-Banja (LL4)	Tuxtuac (LL5)	Mangwendi (LL6)
Olivine	41.54%	40.96%	41.58%	45.23%
Ca-poor-pyroxene	23.22%	29.32%	24.53%	24.89%
Glass	7.48%	9.70%	8.80%	10.25%
Ca-rich-pyroxene	10.81%	3.36%	8.15%	5.32%
Troilite (FeS)	5.19%	5.89%	6.14%	4.59%
Ca-phosphate	0.30%	0.38%	0.07%	0.44%
Chromite	0.25%	0.16%	0.62%	0.35%
Metal	1.72%	0.82%	0.8%	0.5%
Unknown	9.49%	9.74%	9.31%	8.43%